

# Modeling the Hydrodesulfurization Reaction at Nickel. Unusual Reactivity of Dibenzothiophenes Relative to Thiophene and Benzothiophene

David A. Vicic and William D. Jones\*

Contribution from the Department of Chemistry, The University of Rochester, Rochester, New York 14627-0216

Received February 25, 1999

**Abstract:** The nickel hydride dimer [(dippe)NiH]<sub>2</sub> (**1**) was found to react with a variety of organosulfur substrates under mild conditions leading to C–S bond insertion adducts. The transition-metal insertions into the C–S bonds of thiophene, benzothiophene, and dibenzothiophene are all reversible, and lead to new organometallic complexes when dissolved in hydrocarbon solvent. (dippe)Ni( $\eta^2$ -C,S-dibenzothiophene) (**6**) converts to four new organometallic species in a unique desulfurization reaction that is believed to proceed via the intermediacy of the late-metal terminal sulfido complex (dippe)Ni=S (**23**). Independent synthetic routes to the desulfurization products have also provided an entry into the preparation of a variety of nickel–sulfur complexes such as (dippe)Ni(SH)<sub>2</sub>, (dippe)<sub>2</sub>Ni<sub>2</sub>( $\mu$ -H)( $\mu$ -S), [(dippe)<sub>2</sub>Ni<sub>2</sub>( $\mu$ -H)( $\mu$ -S)][PF<sub>6</sub>], and [(dippe)Ni( $\mu$ -S)]<sub>2</sub>, all of which have been structurally characterized. The reactivity of **1** with 4-methyldibenzothiophene, 4,6-dimethyldibenzothiophene, 1,9-dimethyldibenzothiophene, thioxanthene, and thianthrene is also presented.

## Introduction

Raney nickel has seen widespread use in the desulfurization of organic and organometallic compounds.<sup>1</sup> Catalytic desulfurization with Raney nickel under mild laboratory conditions is not feasible, however, because of the chemical inertness of the resulting nickel sulfide that is produced. A catalytic desulfurization agent would not only bring efficiency to synthetic applications, but would also serve as a useful model of the industrial catalysts that are currently used in the hydroprocessing of crude oil. A homogeneous organometallic compound would serve as an excellent model for hydrodesulfurization (HDS) reaction since mechanistic information can be easily extracted by conventional spectroscopic and analytical techniques.<sup>2</sup>

Developing such a model begins with studies on carbon–sulfur bond activation, since the initial C–S bond cleavage represents a fundamental step toward the desulfurization of organic substrates. Previous studies have shown that homogeneous nickel complexes can insert into the carbon–sulfur bonds of aryl thioethers<sup>3</sup> and strained cyclic thioethers,<sup>4</sup> and can also

desulfurize the more stubborn organosulfur compounds such as dibenzothiophene upon acidic workup<sup>5</sup> and in the presence of reducing agents.<sup>6</sup> These results, along with recent successes in platinum HDS modeling studies,<sup>7</sup> encouraged us to prepare a new nickel hydride complex and examine the reactivity of this reagent toward carbon–sulfur bond activation in thiophenic molecules.<sup>8</sup>

## Results and Discussion

**Preparation of a New Nickel Hydride Dimer.** Dinuclear nickel hydride complexes were first prepared almost 30 years ago by Jonas and Wilke. A variety of nickel hydride dimers were synthesized by reaction of L<sub>2</sub>NiCl<sub>2</sub> with 2 equiv of Na[HBMe<sub>3</sub>] (L<sub>2</sub> = chelating bisphosphine ligand).<sup>9</sup> It was found that [(dcpe)NiH]<sub>2</sub> (dcpe = 1,2-bis(dicyclohexylphosphino)ethane) was thermally very stable, and decomposed only in boiling mesitylene. However, this dimer was also found to be chemically quite reactive. Hydrogen was replaced in this system under mild conditions by treatment with triphenylphosphine, a variety of olefins, and benzonitrile to generate (dcpe)NiL<sub>2</sub>

(1) See for example: (a) Pizey, J. S. *Synthetic Reagents*; Wiley: New York, 1974; Vol. 2, p 175. (b) Spera, M. L.; Harman, W. D. *J. Am. Chem. Soc.* **1997**, *119*, 8843. (c) Capozzi, G.; Dios, A.; Franck, R. W.; Geer, A.; Marzabadi, C.; Menichetti, S.; Nativi, C.; Tamarez, M. *Angew. Chem., Int. Ed. Engl.* **1996**, *35*, 777.

(2) See, for example: (a) Curtis, M. D.; Druker, S. H. *J. Am. Chem. Soc.* **1997**, *119*, 1027. (b) Harris, S. *Polyhedron* **1997**, *16*, 3219. (c) Sánchez-Delgado, R. A. *J. Mol. Catal.* **1994**, *86*, 287. (d) Bianchini, C.; Meli, A. *J. Chem. Soc., Dalton Trans.* **1996**, 801. (e) Stafford, P. R.; Rauchfuss, T. B.; Verma, A. K.; Wilson, S. R. *J. Organomet. Chem.* **1996**, *526*, 203. (f) Bianchini, C.; Meli, A. *Acc. Chem. Res.* **1998**, *31*, 109. (g) Zhang, X.; Dullaghan, C. A.; Carpenter, G. B.; Sweigart, D. W.; Meng, Q. *Chem. Commun.* **1998**, 93. (h) Angelici, R. J. *Polyhedron* **1997**, *16*, 3073. (i) Sargent, A. L.; Titus, E. P. *Organometallics* **1998**, *17*, 65. (j) Matsubara, K.; Okamura, R.; Tanaka, M.; Suzuki, H. *J. Am. Chem. Soc.* **1998**, *120*, 1108. (k) Reynolds, J. G. *Chem. Ind.* **1991**, 570. (l) Lopez, L.; Godziela, G.; Rakowski DuBois, M. *Organometallics* **1991**, *10*, 2660.

(3) (a) Osakada, K.; Maeda, M.; Nakamura, Y.; Yamamoto, T.; Yamamoto, A. *J. Chem. Soc., Chem. Commun.* **1986**, 442. (b) Wenkert, E.; Shepard, M. E.; McPhail, A. T. *J. Chem. Soc., Chem. Commun.* **1986**, 442.

(4) Matsunaga, P. T.; Hillhouse, G. L. *Angew. Chem., Int. Ed. Engl.* **1994**, *33*, 1748.

(5) Eisch, J. J.; Hallenbeck, L. E.; Han, K. I. *J. Org. Chem.* **1983**, *48*, 2963.

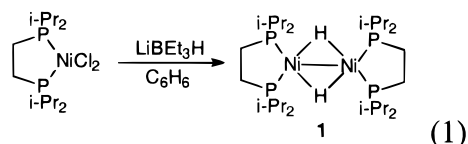
(6) (a) Eisch, J. J.; Hallenbeck, L. E.; Han, K. I. *J. Am. Chem. Soc.* **1986**, *108*, 7763. (b) Becker, S.; Fort, Y.; Vanderesse, R.; Caubère, P. *J. Org. Chem.* **1989**, *54*, 4848. (c) Eisch, J. J.; Hallenbeck, L. E.; Han, K. I. *J. Org. Chem.* **1983**, *48*, 2963. (d) Becker, S.; Fort, Y.; Vanderesse, R.; Caubère, P. *Tetrahedron Lett.* **1988**, *29*, 2963. (e) Kuehm-Caubère, C.; Guilmar, A.; Adach-Becker, S.; Caubère, P. *Tetrahedron Lett.* **1998**, *39*, 8987.

(7) (a) Garcia, J. J.; Maitlis, P. M. *J. Am. Chem. Soc.* **1993**, *115*, 12200. (b) Garcia, J. J.; Mann, B. E.; Adams, H.; Bailey, N. A.; Maitlis, P. M. *J. Am. Chem. Soc.* **1995**, *117*, 2179. (c) Iretskii, A.; Adams, H.; Garcia, J. J.; Picazo, G.; Maitlis, P. M. *Chem. Commun.* **1998**, 61.

(8) A preliminary account of this work has been reported: Vicic, D. A.; Jones, W. D. *J. Am. Chem. Soc.* **1997**, *119*, 10855.

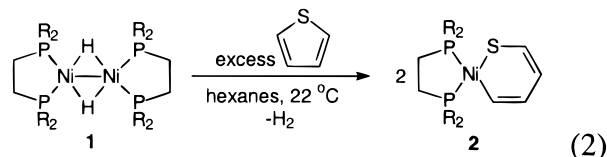
(9) Jonas, K.; Wilke, G. *Angew. Chem., Int. Ed. Engl.* **1970**, *9*, 312.

complexes. We were attracted by both the reactive nature of this hydride dimer and its thermal stability in solution. Specifically, we imagined it would be an excellent desulfurization reagent, since the presence of two reactive metal centers could lead to cleavage of *both* carbon–sulfur bonds of various organic substrates. We chose to prepare a modified version of the cyclohexylphosphine derivative, namely [(dippe)NiH]<sub>2</sub> (**1**) (dippe = 1,2-bis(diisopropylphosphino)ethane), to aid in crystallization efforts. **1** was prepared in 90% yield by addition of 2 equiv of Li[HBET<sub>3</sub>] to a benzene suspension of (dippe)NiCl<sub>2</sub> in benzene (eq 1).<sup>8</sup> The <sup>1</sup>H NMR spectrum of **1** (C<sub>6</sub>D<sub>6</sub>) shows the



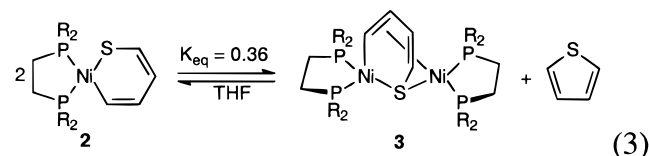
characteristic quintet at  $\delta -9.81$  ( $J = 24.2$  Hz), indicative of the hydride coupling to four equivalent phosphorus atoms. **1** was isolated as a deep red oil and can be kept for months at  $-30$  °C with no apparent decomposition.

**Reactions with Thiophene and Benzothiophene.** Reaction of **1** with excess thiophene in hexanes solution (22 °C) led to the precipitation of a bright yellow solid that could be isolated in analytically pure form by mere filtration. Spectroscopic and analytical data suggested that the product was mononuclear in nature, consistent with an asymmetric ring-opened structure (eq 2). X-ray quality crystals were grown by layering a cold ( $-30$



°C) solution of **2** in CH<sub>2</sub>Cl<sub>2</sub> with hexanes. **2** crystallizes in the rhombohedral space group *R3c*, and is disordered with respect to the orientation of the metallathiabenzene ring. A successful refinement of each orientation was accomplished in SHELX by using bond distance restraints to make each of the rings similar. Related disorders were found for rhodium–thiophene<sup>10</sup> and rhodium–selenophene<sup>11</sup> complexes and were successfully refined by using analogous procedures. The metallacycle adopts a planar conformation, with bond lengths (Å) around the ring for Ni–C(1A), C1A–C2A, C2A–C3A, C3A–C4A, Ni–S(1A), and C(4A)–S(1A) of 1.923(10), 1.363(12), 1.397(11), 1.339(13), 2.152(2), and 1.718(9), respectively, in the thiametallacycle (molecule A is typical). An ORTEP drawing of the single-crystal X-ray structure of **2** is shown in Figure 1.

Although **2** is stable indefinitely in the solid state under inert atmosphere, solutions of **2** quickly turn from yellow to brown, and the appearance of a new product (**3**) with large upfield shifts for the thienyl protons could be seen in the <sup>1</sup>H NMR spectrum, along with the loss of free thiophene (eq 3). Elemental analysis



(10) Blonski, C.; Myers, A. W.; Palmer, M.; Harris, S.; Jones, W. D. *Organometallics* **1997**, *16*, 3819.

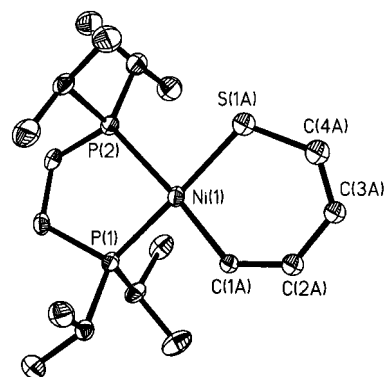
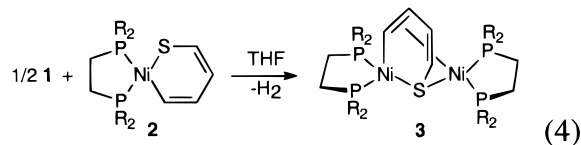


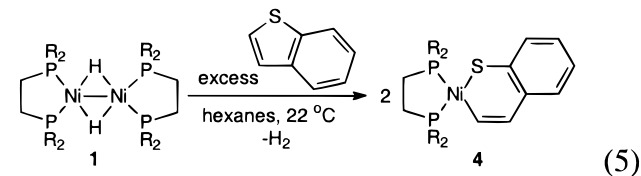
**Figure 1.** ORTEP drawing of (dippe)Ni( $\eta^2$ -C,S-thiophene), **2**. Selected bond lengths (Å): Ni(1)–S(1A), 2.152(2); Ni(1)–C(1A), 1.923(10); C(1A)–C(2A), 1.363(12); C(2A)–C(3A), 1.397(11); C(3A)–C(4A), 1.339(13); C(4A)–S(1A), 1.718(9); Ni(1)–P(1), 2.189(2); Ni(1)–P(2), 2.215(2).

is consistent with the new product being dinuclear in nature, and having incorporated one molecule of thiophene. Consistent with this assignment, four inequivalent phosphine signals could be detected in the <sup>31</sup>P{<sup>1</sup>H} spectrum at low temperature. The formation of **3** is a reversible process, as **3** reverts back to **2** with the addition of excess thiophene. The attainment of equilibrium for eq 3 is rapid at ambient temperature (19 h) and  $K_{eq}$  is 0.36. Dinuclear complex **3** can also be independently prepared by reacting the nickel hydride dimer **1** with the C–S insertion complex **2** (eq 4) in THF. Although in this case **2** was



reactive toward another equivalent of nickel fragment, the addition of excess metal did not lead to the cleavage of the second C–S bond of thiophene.

Benzothiophene has two different carbon–sulfur bonds into which a metal can insert, and we were interested to see if there would be any selectivity by **1**.<sup>12</sup> The nickel insertion complex (dippe)Ni( $\eta^2$ -C,S-benzothiophene) (**4**) was prepared by reaction of **1** with excess benzothiophene in hexanes solution at room temperature (eq 5). The benzothiophene adduct **4** selectively



precipitated from solution, and the bright yellow material was used to grow X-ray quality crystals. X-ray crystallographic analysis revealed a nearly planar metallacycle, which again showed a disorder with respect to the orientation of the thiametallacycle. A similar disorder of a benzothiophene ligand has been seen for Cp\**Rh*(PMe<sub>3</sub>)( $\eta^2$ -C,S-benzothiophene) and was modeled the same way in the present structure.<sup>10</sup> An ORTEP drawing of the single-crystal X-ray structure of **4** is shown in Figure 2. The solid-state structure confirms that metal

(11) Vicic, D. A.; Myers, A. W.; Jones, W. D. *Organometallics* **1997**, *16*, 2751.

(12) For a paper that focuses on the preference of transition-metal complexes for the C–S bonds of benzothiophene see: Palmer, M.; Rowe, S.; Harris, S. *Organometallics* **1998**, *17*, 3798.

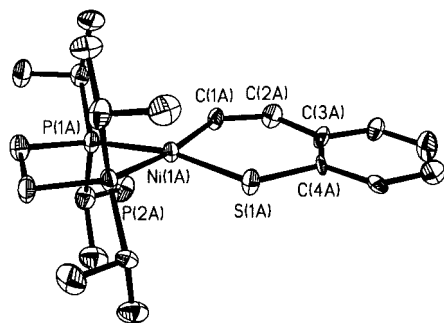


**Figure 2.** ORTEP drawing of (dippe)Ni( $\eta^2$ -C,S-benzothiophene), **4**. Selected bond lengths (Å): Ni(1A)–S(1A), 2.131(4); Ni(1A)–C(1A), 1.910(14); C(1A)–C(2A), 1.34(2); C(2A)–C(3A), 1.43(2); C(3A)–C(4A), 1.39(2); C(4A)–S(1A), 1.758(14); Ni(1A)–P(1A), 2.152(4); Ni(1A)–P(2A), 2.219(4).

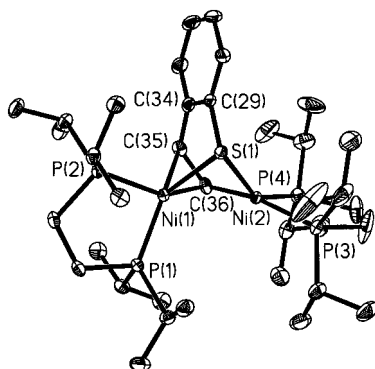
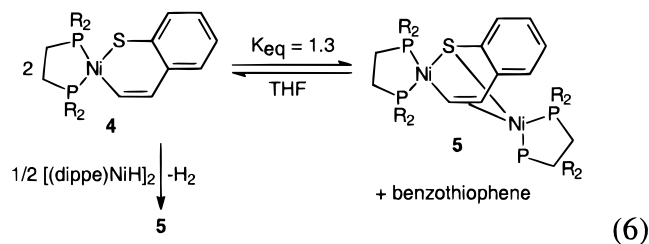


**Figure 3.** ORTEP drawing of (dippe)<sub>2</sub>Ni<sub>2</sub>(benzothiophene), **5**. Selected bond lengths (Å): Ni(1)–S(1), 2.3634(7); Ni(2)–S(1), 2.2630(7); Ni(1)–C(36), 1.985(2); Ni(1)–C(35), 2.142(2); Ni(2)–C(36), 1.908(2); C(35)–C(36), 1.373(4); Ni(1)–P(1), 2.1567(7); Ni(1)–P(2), 2.1836(7); Ni(2)–P(3), 2.2355(7); Ni(2)–P(4), 2.1296(7); Ni(1)–Ni(2), 2.7035(4).

insertion takes place exclusively into the vinyl C–S bond of benzothiophene, and NMR spectroscopy supports the fact that there is no insertion into the aryl C–S bond.<sup>13</sup>

Just as in the case of the thiophene adduct, carbon–sulfur bond cleavage of benzothiophene is reversible. In THF solution, **4** is in equilibrium with the dark green dinuclear species (**5**) (eq 6). Approach to equilibrium was slow in this case (ca. 12



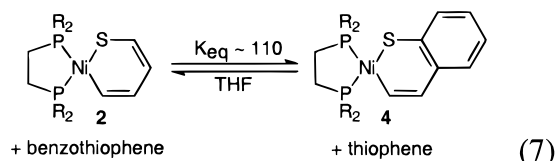
days), and  $K_{eq}$  was found to be  $\sim 1.3$ , in favor of the dinuclear species. **5** was independently prepared by reacting **4** with **1**, and X-ray crystallographic analysis revealed the nature of the dinuclearity. The ORTEP drawing of **5** is shown in Figure 3. The solid-state structure consists of a distorted molecule of **4** in which a second nickel fragment coordinates to the sulfur atom and olefinic bond of **4**. The resulting thiametallacycle no longer adopts a planar configuration, and the benzothiophene ligand

(13) Only two examples of metal insertion into the aryl C–S bond of a benzothiophene have been reported. See: (a) Myers, A. W.; Jones, W. D. *J. Am. Chem. Soc.* **1995**, *117*, 11704. (b) Dullaghan, C. A.; Sun, S. H.; Carpenter G. B.; Weldon B.; Sweigart D. A. *Angew. Chem., Int. Ed. Engl.* **1996**, *35*, 212.

bisects the two metal centers. The Ni–Ni distance in **5** is 2.704 Å, well beyond that of normal Ni–Ni single bonds.<sup>14</sup> Here again, no cleavage of the second carbon–sulfur bond was observed upon addition of excess nickel, and **5** is stable even at temperatures up to 70 °C.

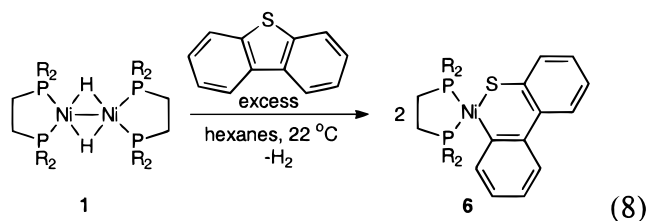
Both the nickel–thiophene and nickel–benzothiophene dinuclear complexes were found to be fluxional in solution. In the <sup>31</sup>P NMR spectra, two of the four resonances for **3** appear to exchange sites, with an apparent coalescence temperature of 30 °C. In contrast, all four of the resonances for **5** coalesced to a broad singlet at 85 °C. At higher temperatures, the resonance for **5** did not sharpen, but rather decomposition took place. Consequently, the origin of the fluxional processes could not be deduced. Fluxional behavior has also been seen in dinuclear cobalt–thiophene<sup>15</sup> and iron–benzothiophene<sup>16</sup> complexes involving a “flip-flop” of the  $\eta^2$ -coordinated double bond from one metal center to the other.

Reaction of **2** with benzothiophene led to the equilibrium shown in eq 7. Only an approximate value for  $K_{eq}$  could be

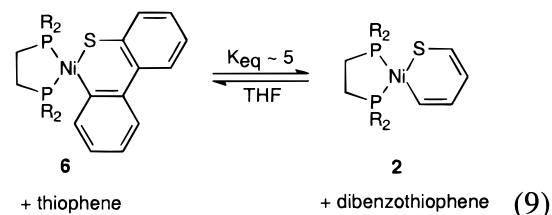


obtained ( $K_{eq} \approx 110$ ), as the dimer **5** slowly grows in over time. The presence of **3** is not observed at equilibrium due to the large ratio of thiophene to **2**. This approximation shows that the benzothiophene adduct **4** is thermodynamically much more stable than the thiophene adduct **2**, for reasons which are not yet clear. Similar results have been found with a platinum–triethylphosphine system, but the (PEt<sub>3</sub>)<sub>2</sub>Pt( $\eta^2$ -C,S-benzothiophene) was found to be only 10 times more stable than (PEt<sub>3</sub>)<sub>2</sub>Pt( $\eta^2$ -C,S-thiophene).<sup>7b</sup>

**Reactions with Dibenzothiophene.** We previously reported that **1** reacts with dibenzothiophene at room temperature to yield the C–S insertion complex **6** (eq 8).<sup>8</sup> The carbon–sulfur bond



insertion into dibenzothiophene is reversible, for dissolution of **6** in neat thiophene at 22 °C leads to quantitative production of the exchange product **2** with the formation of free dibenzothiophene. A rough approximation could be made for the equilibrium between the thiophene and dibenzothiophene adducts ( $K_{eq} \sim 5$ , eq 9), for the dibenzothiophene slowly undergoes



a desulfurization reaction over time (see below). The overall

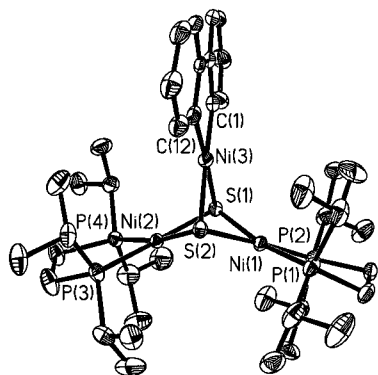
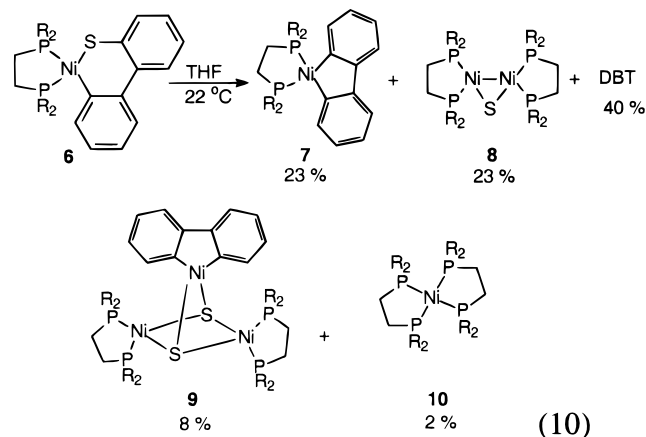


**Figure 4.** ORTEP drawing of  $(\text{dippe})_2\text{Ni}_3(\mu\text{-S})_2(2,2'\text{-biphenyl})$ , **9**. Selected bond lengths (Å): Ni(1)–S(1), 2.194(2); Ni(2)–S(1), 2.201(2); Ni(1)–S(2), 2.192(2); Ni(2)–S(2), 2.191(2); Ni(3)–S(1), 2.238(2); Ni(3)–S(2), 2.233(2); Ni(3)–C(1), 1.916(6); Ni(3)–C(12), 1.919(6); Ni(1)–P(1), 2.158(2); Ni(1)–P(2), 2.159(2); Ni(2)–P(3), 2.161(2); Ni(2)–P(4), 2.163(2); Ni(1)–Ni(2), 2.9641(9); Ni(1)–Ni(3), 2.8203(10); Ni(2)–Ni(3), 2.7673(10). The fold angle of the basal  $\text{Ni}_2\text{S}_2$  unit is  $130.6^\circ$ .

thermodynamic stabilities for the thiametallacycles at nickel are therefore given as  $5 > 4 \gg 2 > 3 > 6$ .

Upon standing in THF solution, the dibenzothiophene adduct **6** is not in equilibrium with a dinuclear analogue of **3** or **5**, but rather converts to four new organometallic products as detected in the  $^1\text{H}$  and  $^{31}\text{P}\{^1\text{H}\}$  NMR spectra (eq 10).<sup>8</sup> Compounds **7**



and **8** are the major organometallic compounds formed and account for 70% of all of **6** consumed. The percentages are based upon moles of product per mole of **6**, i.e., only 50% yield of **8** or 33% yield of **9** is possible. Free dibenzothiophene is also seen in the reaction (2 equiv per **7** or **8**), consistent with the overall stoichiometry of the major products.

The first structure identified in this desulfurization reaction was the trinuclear nickel complex **9**, which was formed in trace amounts. When a solution of **6** was left standing for weeks at room temperature, the low solubility of **9** in benzene led to its selective crystallization. An ORTEP drawing of this trinuclear species can be seen in Figure 4. The structure shows an unusual bonding arrangement in which 2 sulfur atoms bridge 3 nickel centers. The four-membered ring core is bent<sup>17</sup> with a  $49.3^\circ$  pucker of planes between Ni(1)–S(1)–S(2) and Ni(2)–S(1)–S(2). Most interesting is the fact that the sulfur atoms have displaced a chelating phosphine unit from a nickel center. A

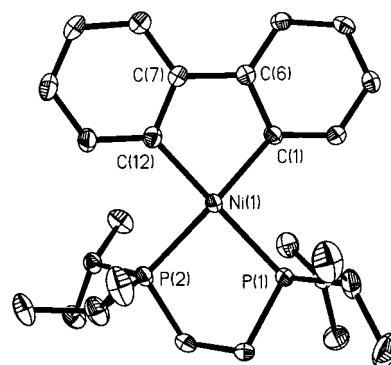


**Figure 5.** ORTEP drawing of  $(\text{dippe})\text{Ni}_2(2,2'\text{-biphenyl})$ , **7**. Selected bond lengths (Å): Ni(1)–C(1), 1.960(3); Ni(1)–C(12), 1.944(3); C(6)–C(7), 1.468(4); Ni(1)–P(1), 2.2142(9); Ni(1)–P(2), 2.2185(9).

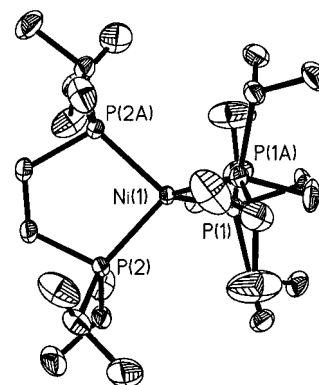


**Figure 6.** ORTEP drawing of  $(\text{dippe})_2\text{Ni}$ , **10**. Selected bond lengths (Å) and angles (deg): Ni(1)–P(1), 2.2096(9); Ni(1)–P(2), 2.2070(8); P(1)–Ni(1)–P(2),  $112.96(3)$ ; P(1)–Ni(1)–P(1A),  $89.88(5)$ ; P(2)–Ni(1)–P(2A),  $90.46(4)$ ; P(1)–Ni(1)–P(2A),  $127.38(3)$ .

mechanistic explanation for the formation of the trinuclear product is presented below.

No free phosphine was detected in the  $^{31}\text{P}\{^1\text{H}\}$  NMR spectrum for the reaction shown in eq 10, despite the fact that trinuclear complex **9** was missing a phosphine unit from one nickel center. The phosphine appears in the nickel tetraphosphine **10** as another minor organometallic compound formed in the desulfurization reaction. Additionally, the major product  $(\text{dippe})\text{-Ni}(2,2'\text{-biphenyl})$  (**7**) was easily identified based on the symmetrical  $^1\text{H}$  NMR resonances for this compound. Independent synthetic routes to **7** and **10** have been developed,<sup>8</sup> which confirmed their identity and allowed easy access to X-ray quality crystals. Complex **7** was prepared by the addition of 2,2'-dilithiobiphenyl to  $(\text{dippe})\text{NiCl}_2$ , and complex **10** was prepared by the addition of free phosphine to **1**. ORTEP drawings of **7** and **10** can be seen in Figures 5 and 6, respectively. **7** displays the expected square-planar geometry for a  $d^8$   $\text{Ni}^{\text{II}}$  complex, whereas **10** displays a tetrahedral  $d^{10}$   $\text{Ni}^0$  structure. The remaining product **8** could not be crystallized from the reaction solution, but was identified by an independent preparation as described below.

**Preparation of Sulfur-Bridged Dinuclear Complexes.** Compound **10** also proved to be a useful precursor to  $(\text{dippe})\text{-}$

(14) See for example: (a) Fryzuk, M. D.; Clentsmith, G. K. B.; Leznoff, D. B.; Rettig, S. J.; Geib, S. J. *Inorg. Chim. Acta* **1997**, *265*, 169. (b) Bach, I.; Goddard, R.; Kopiske, C.; Seevogel, K.; Pörschke, K.-R. *Organometallics* **1999**, *18*, 10.

(15) Jones, W. D.; Chin, R. M. *Organometallics* **1992**, *11*, 2698.

(16) Ogliviy, A. E.; Draganjac, M.; Rauchfuss, T. B.; Wilson, S. R. *Organometallics* **1988**, *7*, 1171.

(17) Aullón G.; Ujaque, G.; Lledós, A.; Alvarez, S.; Alemany P. *Inorg. Chem.* **1998**, *37*, 804.

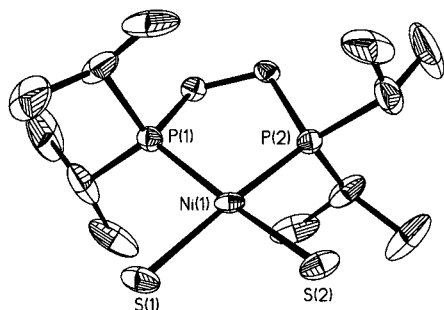
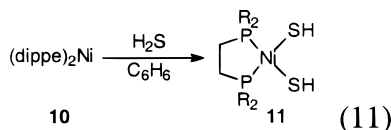


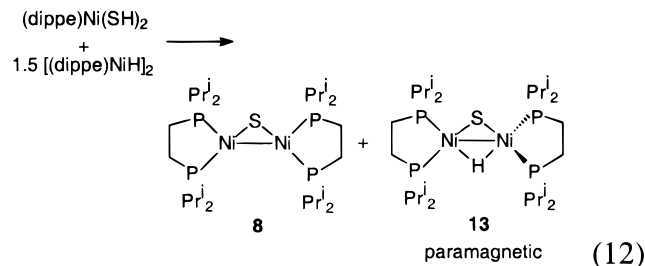
**Figure 7.** ORTEP drawing of (dippe)Ni(SH)<sub>2</sub>, **11**. Selected bond lengths (Å) and angles (deg): Ni(1)–P(1), 2.1670(10); Ni(1)–P(2), 2.1679(10); Ni(1)–S(1), 2.2082(11); Ni(1)–S(2), 2.2065(11); P(1)–Ni(1)–P(2), 88.14(3); S(1)–Ni(1)–S(2), 88.63(4); S(1)–Ni(1)–P(1), 91.94(5); S(2)–Ni(1)–P(2), 92.01(5).

Ni(SH)<sub>2</sub> (**11**, eq 11) when treated with H<sub>2</sub>S. Complex **11** was

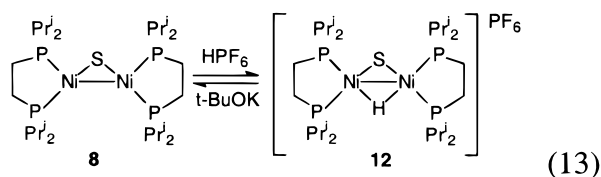


invaluable in the preparation of the sulfur-bridged dimers **8** and **12** (see below). An ORTEP drawing of the single-crystal structure of **11** is shown in Figure 7, displaying the anticipated square-planar geometry with Ni–S bond lengths of 2.207 Å.

For an independent preparation of **8**, 1.5 equiv of **1** was reacted with (dippe)Ni(SH)<sub>2</sub> in THF solvent.<sup>8</sup> This reaction yields not only complex **8** but also the additional paramagnetic complex **13** (eq 12), which was fractionally crystallized by slow



cooling of a pentane solution of the mixture. The major product **8** could not be characterized crystallographically. However, we were able to prepare and fully characterize its protonated derivative **12** which forms upon addition of HPF<sub>6</sub> to a solution of **8**. This reaction is reversible, and **12** can also be deprotonated with potassium *tert*-butoxide to regenerate **8** (eq 13).<sup>8</sup> The



characteristic hydride resonance of **12** appears in the <sup>1</sup>H NMR (THF-*d*<sub>8</sub>) spectrum as a triplet of triplets at δ –11.27 (*J* = 45.6, 25.7 Hz).

Interestingly, **13** differs from the cationic core structure of **12** by only one electron, and in this report we present a rare example in which such electronically related complexes have been structurally characterized.<sup>18</sup> We have found that the one-electron reduction of **12** has a large effect on the geometry of

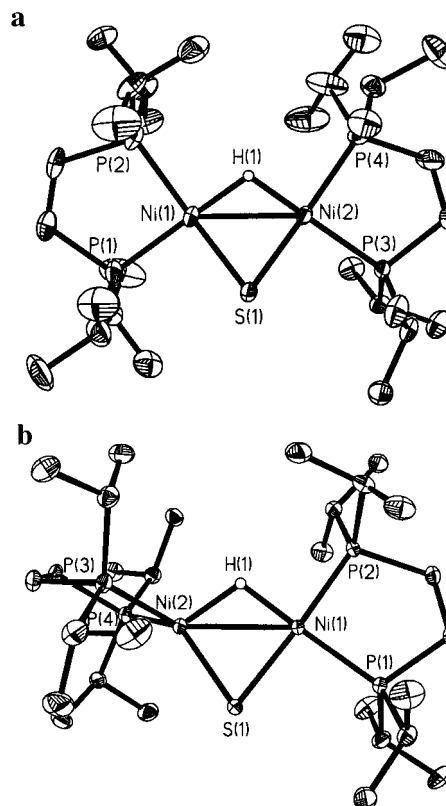


**Figure 8.** (a) ORTEP drawing of the cationic core of **12** (PF<sub>6</sub><sup>–</sup> omitted). The hydride ligand was located and refined isothermally. Selected bond lengths (Å): Ni(1)–Ni(2), 2.5228(8); Ni(1)–S(1), 2.1080(14); Ni(2)–S(1), 2.106(2); Ni(1)–H(1), 1.57; Ni(2)–H(1), 1.53. (b) ORTEP drawing of **13**. The hydride ligand was located and refined isothermally. Selected bond lengths (Å): Ni(1)–Ni(2), 2.5383(3); Ni(1)–S(1), 2.1863(5); Ni(2)–S(1), 2.1266(6); Ni(1)–H(1), 1.57; Ni(2)–H(1), 1.61.

the ground-state species, and have identified the nature of this structural change. ORTEP drawings of both **12** and **13** are shown in Figure 8, parts a and b. **13** can be regarded as a “mixed valence” dimer, containing Ni<sup>II</sup> and Ni<sup>I</sup> centers, with the Ni<sup>II</sup> center adopting a pseudo-square-planar arrangement and the Ni<sup>I</sup> center adopting a pseudo-tetrahedral center. Complex **12**, however, contains two Ni<sup>II</sup> centers, both of which adopt a pseudo-square-planar arrangement. Although the phosphine ligands adopt very different conformations around the metal centers, the Ni–Ni bond lengths in **12** and **13** remain comparable (2.5228(8) and 2.5383(3) Å in **12** and **13**, respectively). In preliminary studies of these dinuclear complexes, we were able to measure a quasireversible reduction of **12** to **13** using cyclic voltammetry and found a potential of –2.2 V (vs ferrocene in THF solvent, Figure 9).<sup>19</sup> An in-depth analysis of the electrochemical behavior will be reported elsewhere. Additional support for the formulation of **13** as a paramagnetic compound lies in the absence of a <sup>1</sup>H or <sup>31</sup>P NMR signal for solutions containing isolated **13**.

(18) See, for example: (a) Gaudiello, J. G.; Wright, T. C.; Jones, R. A.; Bard, A. J. *J. Am. Chem. Soc.* **1985**, *107*, 888. (b) Kang, S.-K.; Albright, T. A.; Jones, R. A. *Organometallics* **1985**, *4*, 666. (c) For an in-depth review on how electron transfer is coupled to structural changes in organometallic complexes, see: Geiger, W. E. *Prog. Inorg. Chem.* **1985**, *33*, 275.

(19) For examples of related Ni(II)/Ni(I) potentials, see: (a) Kim, J. S.; Reibenspies, J. H.; Darensbourg, M. Y. *J. Am. Chem. Soc.* **1996**, *118*, 4115. (b) Morgenstern, D. A.; Ferrence, G. M.; Washington, J.; Henderson, J. J.; Rosenhein, L.; Heise, J. D.; Fanwick, P. E.; Kubiak, C. P. *J. Am. Chem. Soc.* **1996**, *118*, 2198. (c) Osterloh, F.; Saak, W.; Pohl, S. *J. Am. Chem. Soc.* **1997**, *119*, 5648.

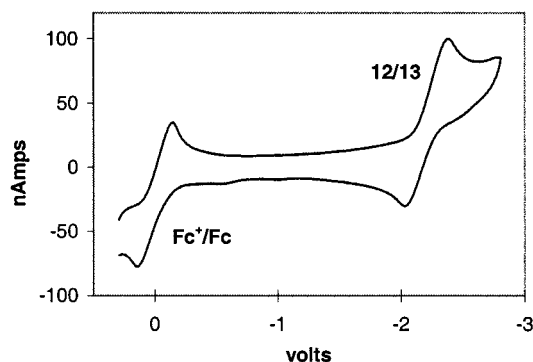


**Figure 9.** Cyclic voltammogram of 3.0 mM **12** in 0.1 M Bu<sub>4</sub>NPF<sub>6</sub>/THF. The sample was referenced versus ferrocene (Fc).

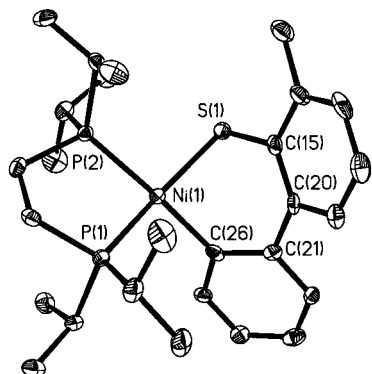


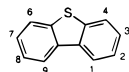
**Figure 10.** ORTEP drawing of (dippe)Ni( $\eta^2$ -C,S-4-methyldibenzothiophene), **14**. Selected bond lengths (Å): Ni(1)–S(1), 2.212(2); Ni(1)–C(26), 1.910(7); C(26)–C(21), 1.422(9); C(21)–C(20), 1.486(9); C(20)–C(15), 1.402(9); C(15)–S(1), 1.783(7); Ni(1)–P(1), 2.172(2); Ni(1)–P(2), 2.212(2).

**Reactions with Alkylated Dibenzothiophenes.** Alkylated dibenzothiophenes, especially those substituted in the 4 and 4,6 positions,<sup>20</sup> are among the least reactive organosulfur compounds found in crude oil distillates. Their HDS rates on standard Co–Mo–Al hydrodesulfurization catalysts are lower by a factor of 10–15 compared with dibenzothiophene,<sup>21</sup> which translates into high temperatures (greater than 380 °C) for the desulfurization process.<sup>22</sup> With a growing demand for “deep” HDS, or production of gas oils with less than 0.05% sulfur content by weight, there is much interest in understanding the structure/reactivity differences of dibenzothiophene, 4-methyldibenzothiophene, and 4,6-dimethyldibenzothiophene.<sup>23</sup> We were therefore interested in exploring the reactivity of **1** toward alkylated dibenzothiophenes.

Reaction of **1** with 4-methyldibenzothiophene at room temperature led to the formation of (dippe)Ni( $\eta^2$ -C,S-4-methyldibenzothiophene) (**14**) in 26% isolated yield. Because of the high lability of the 4-methyldibenzothiophene ligand, all manipulations of **14** had to be done at low temperatures. An X-ray crystallographic analysis of **14** (Figure 10) showed an extremely low biphenyl twist of 28.9°, which presumably arises from steric interactions of the dippe ligand with the methylated ring of the dibenzothiophene unit.<sup>23a</sup>

Like **6**, dissolution of **14** in THF solvent led to a desulfurization reaction. However, the major products formed in this

(20) The numbering scheme for dibenzothiophene is:



(21) (a) Houalla, M.; Broderick, D. H.; Sapre, A. V.; Nag, N. K.; de Beer, V. H. J.; Gates, B. C.; Kwart, H. *J. Catal.* **1980**, *61*, 523. (b) Ma, X.; Sakanishi, K.; Mochida, I. *Ind. Eng. Chem. Res.* **1995**, *34*, 748.

(22) (a) Ishihara, A.; Tajima, H.; Kabe, T. *Chem. Lett.* **1992**, 669. (b) Landau, M. V.; Berger, D.; Herskowitz, M. *J. Catal.* **1996**, *158*, 236.

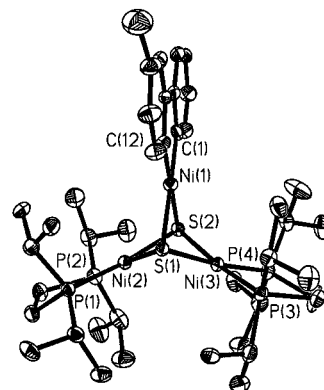
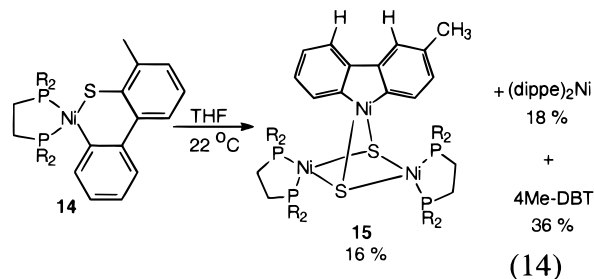
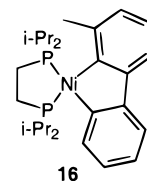


**Figure 11.** ORTEP drawing of rearranged product **15**. Selected bond lengths (Å): Ni(1)–S(1), 2.248(3); Ni(2)–S(1), 2.197(3); Ni(1)–S(2), 2.237(3); Ni(2)–S(2), 2.198(3); Ni(3)–S(1), 2.201(3); Ni(3)–S(2), 2.198(3); Ni(1)–C(1), 1.933(11); Ni(1)–C(12), 1.934(11); Ni(2)–P(1), 2.155(3); Ni(2)–P(2), 2.160(3); Ni(3)–P(3), 2.163(3); Ni(3)–P(4), 2.160(3); Ni(1)–Ni(2), 2.871(2); Ni(1)–Ni(3), 2.840(2); Ni(2)–Ni(3), 2.880(2). The fold angle of the basal Ni<sub>2</sub>S<sub>2</sub> unit is 123.6°.

reaction are trinuclear species **15** and nickel tetraphosphine **10** (eq 14), formed in 16 and 18% yields, respectively. Free



4-methyldibenzothiophene was also formed in the reaction (36%), as well as 30% of intractable material that could not be identified. The trinuclear complex **15** was a completely unexpected product, since the location of the alkyl group implies a rearrangement process with hydride migration. The location of the methyl group can be identified both by <sup>1</sup>H NMR spectroscopy (singlet for the proton atom adjacent to the methyl group on the arene ring) and by X-ray crystallography (Figure 11). Since the reaction proceeds from complex **14** as the starting material, it can be ruled out that **15** arises from any impurities present from the synthesis of 4-methyldibenzothiophene.<sup>24</sup> Heteroatom-promoted C–H activation has been observed with nickel,<sup>25</sup> and may partially account for this unusual rearrangement process. The fact that a nickel–biphenyl complex such as **16** was not observed by NMR spectroscopy may also suggest

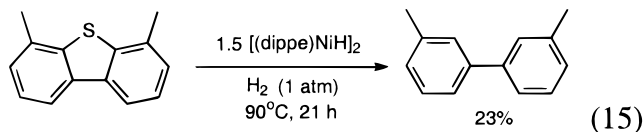


that such a complex is thermally unstable and may rapidly

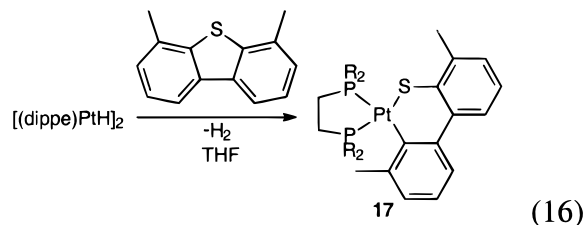
(23) (a) Vivic, D. A.; Jones, W. D. *Organometallics* **1998**, *17*, 3411. (b) Myers, A. W.; Jones, W. D. *Organometallics* **1996**, *15*, 2905. (c) Bianchini, C.; Casares, J. A.; Masi, D.; Meli, A.; Pohl, W.; Vizza, F. *J. Organomet. Chem.* **1997**, *541*, 143. (d) Iretskii, A.; García, J. J.; Picazo, G.; Maitlis, P. M. *Catal. Lett.* **1998**, *51*, 129. (e) Unzelmann, G. H. *Oil Gas J.* **1987**, *June* *19*, 55. (f) Takatsuka, T.; Wada, Y.; Suzuki, H.; Komatsu, S.; Morimura, Y. *J. Jpn. Pet. Inst.* **1992**, *35*, 179. (g) Topsøe, H.; Gates, B. C. *Polyhedron* **1997**, *16*, 3212. (h) Jones, W. D.; Vivic, D. A.; Chin, R. M.; Roache, J. H.; Myers, A. W. *Polyhedron* **1997**, *18*, 3115. (i) Arévalo, A.; Bernès, S.; García, J. J.; Maitlis, P. M. *Organometallics* **1999**, *18*, 1680.

undergo further chemistry leading to **15**. Further investigation of this rearrangement process is underway.

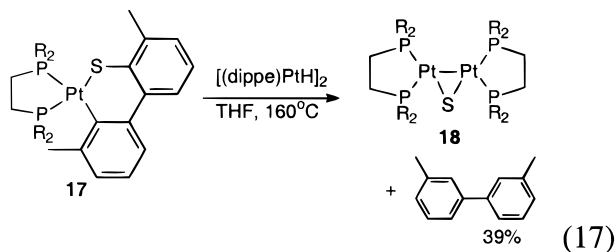
Nickel-hydride **1** did not react with dibenzothiophene substituted in the 4 and 6 positions under mild, room-temperature conditions. However, when 4,6-dimethyldibenzothiophene is heated to 90 °C in the presence of **1** (1.5 equiv in THF), the desulfurized 3,3'-dimethylbiphenyl is produced in 23% yield (eq 15).<sup>23a</sup> A C–S insertion adduct similar to **6** and **14** could



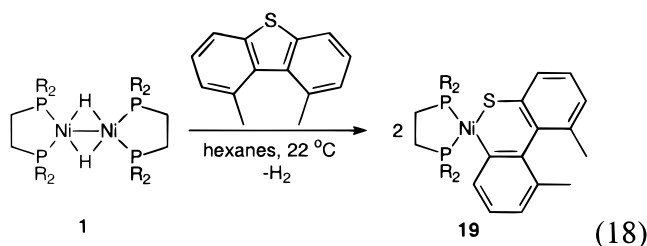
not be detected by NMR spectroscopy, but rather decomposition occurred at these elevated temperatures producing **10** as the only observable product. Nevertheless, control experiments suggest that the desulfurization of 4,6-dimethyldibenzothiophene is homogeneous in nature, and probably proceeds via an initial C–S insertion adduct.<sup>23a</sup> The platinum analogue of **1**, [(dippe)PtH]<sub>2</sub>, was found to produce the first stable insertion adduct of this stubborn substrate (eq 16), and the resulting thiametallacycle



has been structurally characterized. Platinum complex **17** was then found to undergo a desulfurization reaction similar to the nickel adducts when heated in the presence of excess metal hydride (eq 17).<sup>23a</sup>



Reaction of **1** with 1,9-dimethyldibenzothiophene leads to the rapid formation of (dippe)Ni(η<sup>2</sup>-C,S-1,9-dimethyldibenzothiophene) (**19**) (eq 18). The sharp inequivalent signals for all <sup>1</sup>H



NMR resonances for the isopropyl groups indicate that the metallacycle does not undergo a fluxional inversion process on the NMR time scale. This contrasts with the <sup>1</sup>H NMR spectra

(24) Kuehm-Caubère, C.; Adach-Becker, S.; Fort, Y.; Caubère, P. *Tetrahedron* **1996**, 52, 9087.

(25) Kleiman, J. P.; Dubeck, M. *J. Am. Chem. Soc.* **1963**, 85, 1544.

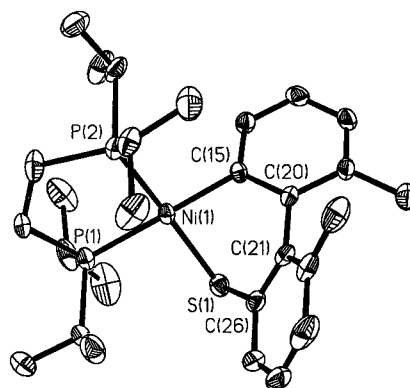
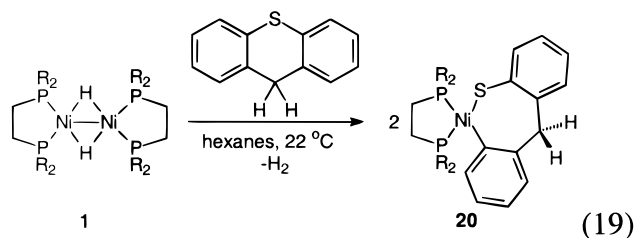


**Figure 12.** ORTEP drawing of (dippe)Ni(η<sup>2</sup>-C,S-1,9-dimethyldibenzothiophene), **19**. Selected bond lengths (Å): Ni(1)–S(1), 2.226(2); Ni(1)–C(15), 1.932(7); C(20)–C(15), 1.414(10); C(21)–C(20), 1.488(11); C(26)–C(21), 1.418(11); C(26)–S(1), 1.781(9); Ni(1)–P(1), 2.211(2); Ni(1)–P(2), 2.156(2).

seen for **6** and **14**, which are broad and unresolved at room temperature. An X-ray analysis of **19** revealed the largest biphenyl twist (53.0°) ever seen for a transition-metal insertion complex of a dibenzothiophene (Figure 12). Interestingly, the carbon–sulfur bond insertion into 1,9-dimethyldibenzothiophene is not reversible, and **19** is stable indefinitely in hydrocarbon-solvents at room temperature. The irreversible nature of this insertion can stem from the fact that a planar transition state leading to reductive elimination may be sterically inaccessible for **19** because of the 1,9-dimethyl interactions. More likely, however, release of free 1,9-dimethyldibenzothiophene may be thermodynamically unfavorable. Examples of 1,9-disubstituted dibenzothiophenes that have been structurally characterized show strained ring systems twisted from planarity because of the 1,9-interactions in the ground state.<sup>26</sup>

**Reaction with Thioxanthene and Thianthrene.** Thioxanthenes and derivatives have been used in heterogeneous HDS studies to gain insight on reaction networks in the hydroprocessing of crude oil.<sup>27</sup> The lone pairs on the sulfur atoms in these compounds are localized with the sulfur atoms relatively exposed, and can therefore be desulfurized quite readily. Such compounds are interesting to compare with planar dibenzothiophenes, since information concerning the interaction of the aromatic rings, as well as the sulfur atoms, with the catalyst can be extracted. Despite the interest shown in heterogeneous studies, there are few examples of homogeneous HDS model studies that use thioxanthenes or thianthrenes as organosulfur substrates.<sup>6</sup> Here we report that the dinuclear nickel-hydride **1** reacts readily with thioxanthene affording (dippe)Ni(η<sup>2</sup>-C,S-thioxanthene) (**20**) (eq 19). The resulting thiametallacycle has



been structurally characterized, and an ORTEP drawing can be

(26) Staab, H. A.; Höne, M.; Krieger, C. *Tetrahedron Lett.* **1988**, 29, 1905.

(27) (a) Girgis, M. J.; Gates, B. C. *Ind. Eng. Chem. Res.* **1991**, 30, 2021. (b) Singhal, G. H.; Espino, R. L.; Sobel, J. E. *J. Catal.* **1981**, 67, 446. (c) Badger, G. M.; Cheuychit, P.; Sasse, W. H. F. *Aust. J. Chem.* **1964**, 17, 366. (d) Benjamin, B.; Raaen, V.; Maupin, P.; Brown, L.; Collins, C. *Fuel* **1978**, 57, 269.

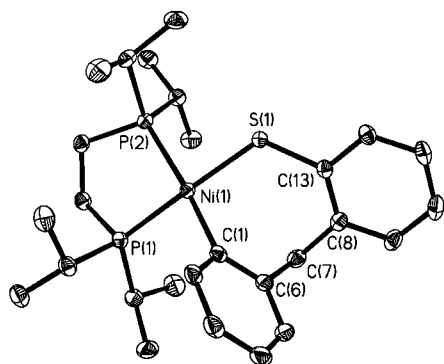


**Figure 13.** ORTEP drawing of (dippe)Ni( $\eta^2$ -C,S-thioxanthene), **20**. Selected bond lengths (Å): Ni(1)–S(1), 2.1903(9); Ni(1)–C(1), 1.930(3); C(1)–C(6), 1.397(5); C(6)–C(7), 1.513(5); C(7)–C(8), 1.515(5); C(8)–C(13), 1.397(4); C(13)–S(1), 1.762(3); Ni(1)–P(1), 2.1788(9); Ni(1)–P(2), 2.2361(9).

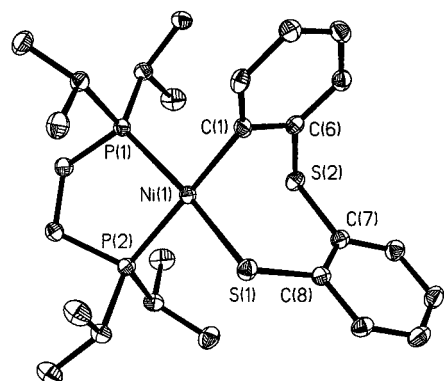
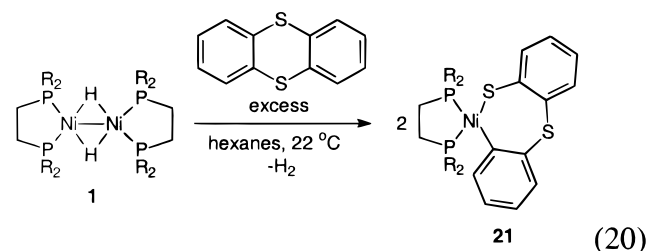


**Figure 14.** ORTEP drawing of (dippe)Ni( $\eta^2$ -C,S-thianthrene), **21**. Selected bond lengths (Å): Ni(1)–S(1), 2.2469(8); Ni(1)–C(1), 1.922(3); S(1)–C(8), 1.755(3); C(8)–C(7), 1.396(4); C(7)–S(2), 1.779(3); S(2)–C(6), 1.780(3); C(6)–C(1), 1.406(4); Ni(1)–P(1), 2.1655(8); Ni(1)–P(2), 2.1957(8).

seen in Figure 13. The metallacycle adopts a puckerred conformation, leading to inequivalent signals for benzylic protons on the thioxanthene ligand ( $\delta$  4.72 (d,  $J$  = 11.0 Hz) and 3.79 (d,  $J$  = 11.0 Hz)).

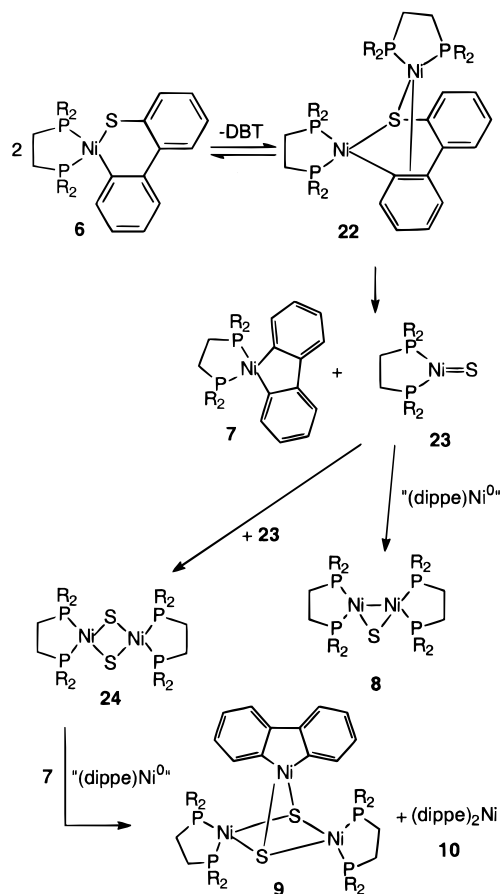
**1** reacts with thianthrene in a similar fashion to yield the C–S insertion complex **21** (eq 20). As shown in the ORTEP drawing



of **21**, the resulting metallacycle (Figure 14) is puckerred in a similar fashion as that of thioxanthene. Sharp signals for all resonances in the  $^1\text{H}$  NMR spectrum for **20** and **21** indicate that the metallacycles are not undergoing inversion on the NMR time scale. The carbon–sulfur bond insertion products of thioxanthene and thianthrene were not in equilibrium with dinuclear complexes, and none of the free organosulfur ligand could be detected by NMR spectroscopy even upon standing in THF solution for days.

**Mechanism of Desulfurization of Dibenzothiophene.** An unusual system has been uncovered in which dibenzothiophene undergoes desulfurization readily whereas thiophene and ben-

**Scheme 1.** Proposed Mechanism for the Desulfurization of Dibenzothiophene



zothiophene, under similar conditions, do not. A key reactivity feature found for most of the thiametallacycles in this study is that carbon–sulfur bond cleavage is reversible. In the case of thiophene and benzothiophene, the (dippe)Ni<sup>0</sup> fragment that is produced upon loss of a thiophenic unit has the option of re-adding the free thiophene or forming a dinuclear complex such as **3** or **5**. A similar reaction may be occurring with the dibenzothiophene adduct, but we were unable to detect a species such as **22** (Scheme 1) by NMR spectroscopy. Such an intermediate may be destabilized for several reasons. First, unlike the thiophene and benzothiophene adducts, the dibenzothiophene ligand in **6** does not possess carbon–carbon bonds with isolated double bond character. Additionally, by extrapolation of the X-ray data for **5**, the phenyl group of the dibenzothiophene would be in close proximity to the isopropyl groups of the phosphine ligands. Both of these reasons would, in principle, prevent a dinuclear species such as **22** from having a significant thermodynamic stability, although a dinuclear complex with cobalt ((Cp<sup>\*</sup>Co)<sub>2</sub>( $\eta^2$ -C,S-dibenzothiophene)) is known.<sup>28</sup> This cobalt complex was found to be more fluxional than the analogous dinuclear thiophene complex, however, since  $\eta^2$  coordination of the olefinic portion of the molecule disrupts aromaticity in the dibenzothiophene ligand.

We propose that a transient species such as **22** does indeed form, and may lie en route to a sulfur atom abstraction reaction leading to the production of the observed nickel–biphenyl complex **7** and the novel terminal sulfido complex **23** (Scheme 1). Such a reaction pathway is attractive for it can easily explain the formation of products **8**, **9**, and **10**. Complex **8** could simply

(28) Jones, W. D.; Chin, R. M. *J. Organomet. Chem.* **1994**, *472*, 311.

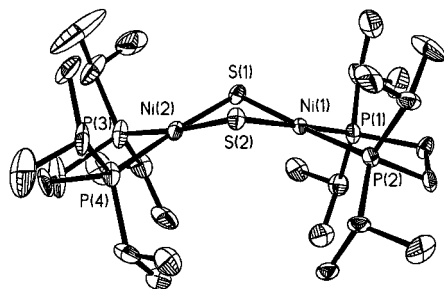
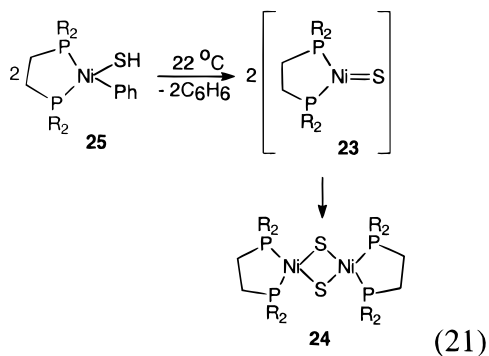
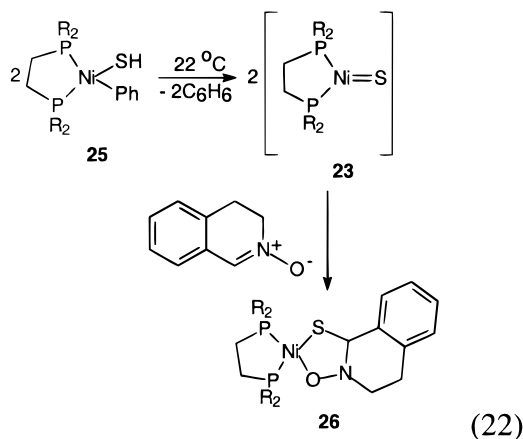


**Figure 15.** ORTEP drawing of  $[(\text{dippe})\text{Ni}(\mu\text{-S})]_2$ , **24**. Selected bond lengths (Å): Ni(1)–S(1), 2.187(3); Ni(2)–S(1), 2.201(4); Ni(1)–S(2), 2.206(3); Ni(2)–S(2), 2.194(3); Ni(1)–P(1), 2.145(3); Ni(1)–P(2), 2.149(3); Ni(2)–P(3), 2.144(4); Ni(2)–P(4), 2.152(4); Ni(1)–Ni(2), 2.941(2). The dihedral angle between the nickel square planes is  $139.3^\circ$ .

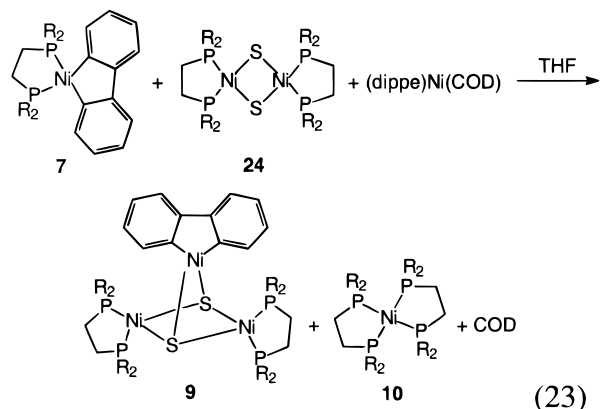
be formed by trapping the sulfido with an additional “Ni<sup>0</sup>” fragment. The stoichiometry of such a pathway is consistent with the fact that we observe roughly 2 equiv of dibenzothiophene per **7** or **8** in eq 10. Such a pathway can also explain the formation of the core structure in trinuclear complex **9** via dimerization of 2 equiv of **23** to give  $[(\text{dippe})\text{Ni}(\mu\text{-S})]_2$  (**24**). To support this hypothesis, we sought to generate a nickel sulfido in situ, and see if a dimerization reaction was possible.<sup>29</sup> We found that thermolysis of  $(\text{dcpe})\text{Ni}(\text{SH})(\text{Ph})$  (**25**) in THF led to the loss of benzene and formation of  $[(\text{dcpe})\text{Ni}(\mu\text{-S})]_2$  in quantitative yield (eq 21) by NMR spectroscopy. A single-crystal



X-ray structure of **24** is shown in Figure 15, showing the bent nature of the Ni<sub>2</sub>(μ-S)<sub>2</sub> linkage.<sup>29</sup> The rate of dimer formation was found to be independent of the concentration of **25**, a result consistent with a unimolecular rate-determining step involving loss of benzene and formation of the terminal sulfido complex. We have also been able to provide structural evidence for a terminal sulfido complex of nickel by trapping a  $(\text{dcpe})\text{Ni}=\text{S}$  complex with 3,4-dihydroisoquinoline *N*-oxide and characterizing the product (**26**) by X-ray crystallography (eq 22).<sup>29</sup>



Having established that a terminal sulfido complex of nickel is chemically feasible and can also form  $\mu$ -sulfido dimers such as **24**, we set out to investigate the pathway for formation of the minor trinuclear product **9**. We have previously reported that reaction of **24** with **7** led to production of **9**, but at a rate that was inconsistent with such a pathway being operative in the desulfurization reaction of **6**.<sup>8</sup> However, when the same reaction is performed in the presence of a Ni<sup>0</sup> complex, **9** is formed quite readily. Reaction of **24** with 1 equiv of **7** and  $(\text{dippe})\text{Ni}(\text{COD})$  led to a 25% production of **9** in 39 h (eq 23). The  $(\text{dippe})\text{Ni}(\text{COD})$  complex does not act as a mere phosphine



sponge in this reaction, for the addition of excess phosphine to **9** results in no reaction. It can therefore be ruled out that **9**, **7**, **24**, and free phosphine are involved in an equilibrium process. Work by Heimbach has previously shown that reaction of a mixture of bisphosphine Ni<sup>0</sup> and Ni<sup>II</sup> complexes affords a disproportionation reaction,<sup>30</sup> and such a pathway might be involved in initiating the formation of the minor products **9** and **10** upon partial conversion of **6** to **7** and **23**. Further precedence for such a reaction has been observed by Eisch and co-workers,<sup>31</sup> who found that thermolysis of a bisphosphine Ni<sup>II</sup> biphenyl complex slowly led to a Ni<sup>I</sup> dimer that could undergo a variety of chemical transformations. Such an unusual process may also be involved in the formation of the rearranged product **15** which resulted from the desulfurization of 4-methyldibenzothiophene. Further experiments are needed, however, to clarify the mechanism of trimer formation in these desulfurization reactions.

## Conclusions

An important point that has emerged from recent HDS modeling studies is that homogeneous desulfurization reactions using late transition metals may involve the formation of transient terminal sulfido complexes.<sup>7b,29,32</sup> Such an observation is important since the details of the mechanism(s) by which heterogeneous catalysts remove sulfur from thiocarbon impurities found in crude oil remains unclear, and late-metal promoter atoms may be critically involved in the sulfur atom abstraction process. The eventual formation of bridged  $\mu$ -sulfido aggregates or terminal M–SH sites under large pressures of H<sub>2</sub> will of course be thermodynamically favored, but it is quite possible that many of these sites originate from initially formed terminal sulfido ligands.

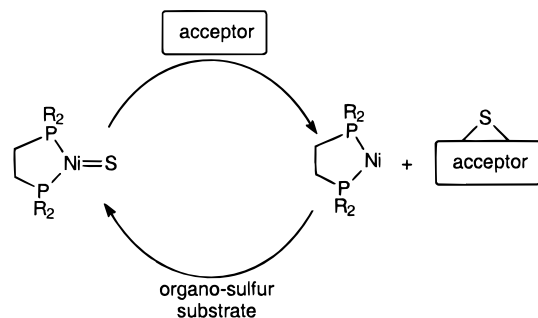
(29) Vicic, D. A.; Jones, W. D. *J. Am. Chem. Soc.* **1999**, *121*, 4070.

(30) Heimbach, P. *Angew. Chem., Int. Ed. Engl.* **1964**, *3*, 648.

(31) Eisch, J. J.; Piotrowski, A. M.; Han, K. I.; Krüger, C.; Tsay, Y. H. *Organometallics* **1985**, *4*, 224.

(32) Bianchini, C.; Jimenez, M. V.; Meli, A.; Moneti, S.; Vizza, F.; Herrera, V.; Sánchez-Delgado, R. *Organometallics* **1995**, *14*, 2342–2352.

**Scheme 2.** A Critical Step in Achieving Homogeneous HDS of Dibenzothiophene for Reactions that Proceed through a Terminal Sulfido Intermediate Will be Sulfur-Atom Transfer To Form Newly Functionalized Compounds or H<sub>2</sub>S



In homogeneous modeling studies, most of the successes of HDS of dibenzothiophenes in the absence of hydride or acid sources have required elevated temperatures and/or high pressures of H<sub>2</sub>.<sup>21,32</sup> These extreme reaction conditions have generally precluded the unambiguous identification of the organometallic products formed in the desulfurization reactions. The ability of **1** to desulfurize dibenzothiophenes at room temperature has provided an opportunity to structurally characterize most of the organometallic products, and has allowed us to speculate on the mechanism of their formation. In this report we show that nickel can desulfurize dibenzothiophenes in the solution phase, and provide evidence that these desulfurizations may be proceeding through an initially formed terminal sulfido intermediate. The consequence of such an intermediate is that *catalytic* desulfurizations in the homogeneous phase may require a rapid sulfur-atom transfer to a sulfur-atom acceptor as shown in Scheme 2. Trapping the sulfido intermediates with hydrogen or other acceptors will be crucial because aggregation to form highly stable bridged  $\mu$ -sulfido complexes may render catalysis unlikely.

## Experimental Procedures

**General Considerations.** All operations were performed under a nitrogen atmosphere unless otherwise stated. THF, pentane, and hexanes were distilled from dark purple solutions of benzophenone ketyl. Thiophene (99+%) was purchased from Aldrich Chemical Co. and purified as previously reported.<sup>33</sup> Benzothiophene was purchased from Aldrich Chemical Co. and used without further purification. A Siemens-SMART 3-Circle CCD diffractometer was used for X-ray crystal structure determination. Elemental analyses were obtained from Desert Analytics. All <sup>1</sup>H, <sup>31</sup>P, and <sup>13</sup>C spectra were recorded on a Bruker AMX400 NMR spectrometer, and all <sup>1</sup>H chemical shifts are reported relative to the residual proton resonance in the deuterated solvent. The syntheses of compounds **1**, **2**, **6**, **7**, **8**, **9**, **10**, and **11** have been previously published in the Supporting Information in ref 8. X-ray structures have been previously reported for **6**,<sup>8</sup> **12**,<sup>8</sup> **14**,<sup>23a</sup> **24**,<sup>29</sup> and **26**,<sup>29</sup> as well as the platinum analogues of **6** and **14**.<sup>23a</sup> Compounds **14**,<sup>23a</sup> **24**,<sup>29</sup> **25**,<sup>29</sup> **26**,<sup>29</sup> and thioxanthene<sup>34</sup> were prepared according to previously reported procedures. Electrochemical studies were carried out under an inert atmosphere with an Analytical Instrument Systems-DLK-60 electrochemical analyzer in a nitrogen drybox. The working electrode was a 125  $\mu$ M platinum disk. A platinum wire served as the auxiliary electrode, and a silver wire served as a pseudoreference electrode. The CV experiments were done in THF at room temperature with ferrocene as an internal standard, 0.1 M in supporting electrolyte (tetra-*n*-butylammonium hexafluorophosphate). The scan rate was 0.5 V/s.

**Preparation of (dippe)<sub>2</sub>Ni( $\eta^2$ -C,S-thiophene) (**3**):** (dippe)Ni( $\eta^2$ -C,S-thiophene) (150 mg, 0.37 mmol) and [(dippe)NiH]<sub>2</sub> (110 mg, 0.17

mmol) were dissolved in THF and stirred at room temperature for 13.5 h. The solvents were removed under vacuum and the product was extracted with pentane. Removal of pentane yielded 210 mg (85%) of a brown solid. <sup>1</sup>H NMR (400 MHz, THF-*d*<sub>8</sub>, 25 °C):  $\delta$  6.64 (t, *J* = 6.3 Hz, 1H), 5.73 (m, 1H), 5.07 (d, *J* = 6.5 Hz, 1H), 4.62 (m, 1H), 2.44–0.85 (m, 64 H). <sup>31</sup>P{<sup>1</sup>H} (toluene-*d*<sub>8</sub>, 10 °C, 162 MHz):  $\delta$  80.84 (d, *J* = 36.6 Hz), 76.2 (dd, *J* = 51.0, 3.3 Hz), 72.45 (dd, *J* = 51.1, 21.1 Hz), 70.56 (dd, *J* = 37.2, 21.1 Hz). Anal. Calcd (found) for C<sub>32</sub>H<sub>68</sub>Ni<sub>2</sub>P<sub>4</sub>S: 52.92 (52.54) C; 9.44 (9.63) H.

**Preparation of (dippe)Ni( $\eta^2$ -C,S-benzothiophene) (**4**):** Benzothiophene (328 mg, 2.5 mmol) was added to a stirred solution of [(dippe)NiH]<sub>2</sub> (200 mg, 0.31 mmol) in hexanes (50 mL) and the solution was stirred at room temperature for 2 h. The yellow precipitate was collected and rinsed with pentane. Yield: 170 mg (61%). <sup>1</sup>H NMR (400 MHz, THF-*d*<sub>8</sub>, 25 °C):  $\delta$  7.70 (d, *J* = 8.2 Hz, 1H), 7.37–7.22 (m, 2H), 7.13 (dd, *J* = 7.3, 1.4 Hz, 1H), 6.89–6.81 (m, 2H), 2.48 (oct, *J* = 7.4 Hz, 2H), 2.37 (oct, *J* = 6.8 Hz, 2H), 1.94 (sext, *J* = 7.9 Hz, 2H), 1.79 (sext, *J* = 7.6 Hz, 2H), 1.38–1.18 m, 24H). <sup>13</sup>C{<sup>1</sup>H} NMR (CD<sub>2</sub>Cl<sub>2</sub>, –40 °C, 100 MHz):  $\delta$  139.39 (dd, *J* = 28.3, 6.9 Hz), 135.10 (s), 133.49 (d, *J* = 12.7 Hz), 132.73 (s), 130.51 (s), 129.30 (d, *J* = 6.2 Hz), 123.88 (s), 120.88 (s), 24.17 (d, *J* = 19.9 Hz), 23.81 (d, *J* = 22.9 Hz), 22.18 (t, *J* = 21.56), 19.56 (dd, *J* = 22.3, 13.5 Hz), 18.78 (s), 18.47 (s), 18.03 (s), 17.85 (s). <sup>31</sup>P{<sup>1</sup>H} (THF-*d*<sub>8</sub>, 25 °C, 162 MHz):  $\delta$  82.56 (d, *J* = 21.8 Hz), 73.62 (d, *J* = 21.5 Hz). Anal. Calcd (found) for C<sub>22</sub>H<sub>38</sub>NiP<sub>2</sub>S: 58.04 (58.18) C; 8.41 (8.28) H.

**Preparation of (dippe)<sub>2</sub>Ni( $\eta^2$ -C,S-benzothiophene) (**5**):** (dippe)Ni( $\eta^2$ -C,S-benzothiophene) (127 mg, 0.28 mmol) and [(dippe)NiH]<sub>2</sub> (95 mg, 0.15 mmol) were dissolved in THF and stirred at room temperature for 1 h. The solvents were removed under vacuum and the product was extracted with pentane. Removal of pentane yielded 169 mg (78%) of a dark green solid. <sup>1</sup>H NMR (400 MHz, THF-*d*<sub>8</sub>, 25 °C):  $\delta$  7.08 (d, *J* = 7.4 Hz, 1H), 6.92 (d, *J* = 7.5 Hz, 1H), 6.53 (dt, *J* = 7.2, 1.4 Hz, 1H), 6.34 (t, *J* = 6.9 Hz, 1H), 5.76 (m, 1H), 4.89 (m, 1H), 2.54–0.66 (m, 64H). <sup>31</sup>P{<sup>1</sup>H} (toluene-*d*<sub>8</sub>, 25 °C, 162 MHz):  $\delta$  80.57 (d, *J* = 22.6 Hz), 72.54 (br s), 65.34 (br s), 59.10 (d, *J* = 21.5 Hz). Anal. Calcd (found) for C<sub>36</sub>H<sub>70</sub>Ni<sub>2</sub>P<sub>4</sub>S: 55.70 (55.81) C; 9.09 (9.26) H.

**Establishing the Equilibrium between **2** and **3** and Thiophene (Eq 3).** (dippe)Ni( $\eta^2$ -C,S-thiophene) (**2**) (7.1 mg, 0.02 mmol) was dissolved in 1.05 mL of THF-*d*<sub>8</sub> and placed into a flame-sealed NMR tube. The solution was kept standing at room temperature until equilibrium was established, and the final *K*<sub>eq</sub> was determined by integrating the thienyl resonances of monomer vs dimer.

**Establishing the Equilibrium between **4** and **5** and Benzothiophene (Eq 5).** (dippe)Ni( $\eta^2$ -C,S-benzothiophene) (**4**) (8.0 mg, 0.02 mmol) was dissolved in 1.05 mL of THF-*d*<sub>8</sub> and placed into a flame-sealed NMR tube. The solution was kept standing at room temperature until equilibrium was established, and the final *K*<sub>eq</sub> was determined by integrating the thienyl resonances of monomer vs dimer.

**Isolation of paramagnetic complex **13**:** **1** (87 mg, 0.14 mmol) and **11** (35 mg, 0.13 mmol) were dissolved in THF and stirred for 15 min. The solvent was removed under vacuum, and the products were extracted with a minimum amount of pentane. The solution was filtered through a glass wool plug, and cooled to –30 °C upon which 6 mg of dark red crystals formed. Isolated yield 7%. Complex **13** is NMR inactive. Anal. Calcd (found) for C<sub>28</sub>H<sub>65</sub>Ni<sub>2</sub>P<sub>4</sub>S: 49.81 (49.22) C; 9.70 (9.29) H.

**Preparation of (dippe)Ni( $\eta^2$ -C,S-4-methyldibenzothiophene) (**14**):** [(dippe)NiH]<sub>2</sub> (60 mg, 0.09 mmol) was added to a stirred solution of 4-methyldibenzothiophene (372 mg, 1.9 mmol) in 20 mL of hexanes. The solution was stirred for 4 h and filtered. The filtrate was collected and to this solution was added 23 mg (0.04 mmol) of [(dippe)NiH]<sub>2</sub>. The solution was then stirred at room temperature for 15.5 h. The resulting orange precipitate was filtered, washed with hexanes, and dried under vacuum. Yield: 35 mg (26%). <sup>1</sup>H NMR (400 MHz, THF-*d*<sub>8</sub>, –30 °C):  $\delta$  7.34 (t, *J* = 6.1 Hz, 1H), 7.28 (d, *J* = 7.8 Hz, 1H), 7.17 (d, *J* = 7.2 Hz, 1H), 6.91–6.82 (m, 2H), 6.80 (t, *J* = 7.1 Hz), 6.75 (t, *J* = 7.4 Hz, 1H), 2.92 (br s, 1H), 2.49 (br s, 1H), 2.42 (s, 3H), 2.17–1.86 (m, 4H), 1.70–1.57 (m, 2H), 1.53 (dd, *J* = 16.0, 6.2 Hz, 3H), 1.31 (dd, *J* = 12.5, 6.3 Hz, 3H), 1.21–1.02 (m, 9H), 0.76 (dd, *J* = 16.9, 7.0 Hz, 3H), 0.27 (dd, *J* = 13.6, 6.7 Hz, 3H). <sup>13</sup>C{<sup>1</sup>H} NMR (CD<sub>2</sub>Cl<sub>2</sub>, –78 °C, 100 MHz):  $\delta$  156.57 (dd, *J* = 24.4, 25.2 Hz), 148.14

(33) Spies, G. H.; Angelici, R. J. *Organometallics* **1987**, *6*, 1897.

(34) Mlotkowska, B. L.; Cushman, J. A.; Harwood, J.; Lam, W. W.; Ternay, A. L. *J. Heterocycl. Chem.* **1991**, *28*, 731.

**Table 1.** Crystallographic Data for Compounds **2**, **4**, **5**, **7**, **9**, and **10**

crystal parameters	<b>2</b>	<b>4</b>	<b>5</b>	<b>7</b>	<b>9</b> ·(2C <sub>6</sub> H <sub>6</sub> )	<b>10</b>
chemical formula	C <sub>18</sub> H <sub>36</sub> NiP <sub>2</sub> S	C <sub>22</sub> H <sub>38</sub> NiP <sub>2</sub> S	C <sub>28</sub> H <sub>44</sub> NiP <sub>2</sub> S	C <sub>26</sub> H <sub>40</sub> NiP <sub>2</sub>	C <sub>40</sub> H <sub>72</sub> Ni <sub>3</sub> P <sub>4</sub> S <sub>2</sub>	C <sub>28</sub> H <sub>64</sub> NiP <sub>4</sub>
formula weight	405.18	455.24	776.28	473.23	917.09	583.38
cryst syst	rhombohedral	monoclinic	monoclinic	monoclinic	monoclinic	monoclinic
space group	<i>R</i> 3 <i>c</i>	<i>C</i> 2/ <i>c</i>	<i>P</i> 2 <sub>1</sub> / <i>n</i>	<i>P</i> 2 <sub>1</sub> / <i>n</i>	<i>C</i> 2/ <i>c</i>	<i>C</i> 2/ <i>c</i>
Z	18	12	4	4	12	4
<i>a</i> , Å	26.9434(3)	26.8030 (20)	11.5365 (2)	8.3256 (3)	35.5706(1)	19.3695(2)
<i>b</i> , Å	26.9434(3)	15.3487(13)	23.5981 (3)	15.3734(5)	20.9896(2)	9.8492(1)
<i>c</i> , Å	15.0018(3)	18.1040(14)	14.7722 (2)	19.3875(6)	19.9602(2)	18.7555(2)
$\beta$ , deg	90	90	90.7210 (10)	95.3090(10)	98.7470(10)	113.0130(10)
vol, Å <sup>3</sup>	9431.5(2)	7407.9(10)	4021.26(10)	2470.81(14)	14729.2(2)	3293.31(6)
temp, °C	-70	-80	-80	-80	-80	-80
<i>R</i> <sub>1</sub> ( <i>F</i> <sub>o</sub> ), <i>wR</i> <sub>2</sub> ( <i>F</i> <sub>o</sub> <sup>2</sup> ) [ <i>F</i> <sub>o</sub> > 4σ( <i>F</i> <sub>o</sub> )]	0.0479, 0.0652	0.1058, 0.2465	0.0336, 0.0766	0.0497, 0.0815	0.0504, 0.1320	0.0444, 0.1148
<i>R</i> <sub>1</sub> ( <i>F</i> <sub>o</sub> ), <i>wR</i> <sub>2</sub> ( <i>F</i> <sub>o</sub> <sup>2</sup> ) [all data]	0.0612, 0.0679	0.1421, 0.2678	0.0400, 0.0797	0.0697, 0.0878	0.0641, 0.1392	0.0512, 0.1190
goodness of fit	1.161	1.139	1.039	1.081	1.141	1.106

**Table 2.** Crystallographic Data for Compounds **11**, **13**, **15**, **19**, **20**, and **21**

crystal parameters	<b>11</b>	<b>13</b>	<b>15</b>	<b>19</b>	<b>20</b>	<b>21</b>
chemical formula	C <sub>14</sub> H <sub>32</sub> P <sub>2</sub> NiS	C <sub>28</sub> H <sub>65</sub> Ni <sub>2</sub> P <sub>4</sub> S	C <sub>41</sub> H <sub>74</sub> Ni <sub>3</sub> P <sub>4</sub> S <sub>2</sub>	C <sub>28</sub> H <sub>44</sub> NiP <sub>2</sub> S	C <sub>27</sub> H <sub>42</sub> NiP <sub>2</sub> S	C <sub>26</sub> H <sub>40</sub> NiP <sub>2</sub> S <sub>2</sub>
formula weight	385.17	675.16	931.13	533.34	519.32	537.35
cryst syst	tetragonal	triclinic	triclinic	monoclinic	monoclinic	monoclinic
space group, Z	<i>I</i> 4, 8	<i>P</i> 1, 2	<i>P</i> 1, 6	<i>P</i> 2 <sub>1</sub> / <i>c</i> , 4	<i>P</i> 2 <sub>1</sub> / <i>c</i> , 4	<i>P</i> 2 <sub>1</sub> / <i>c</i> , 4
<i>a</i> , Å	14.62600(10)	9.0236(1)	20.4729(4)	9.4302(2)	11.4852(2)	10.3177(1)
<i>b</i> , Å	14.62600(10)	12.0684(2)	20.6412(4)	14.8247(1)	15.7422(3)	16.3507(2)
<i>c</i> , Å	18.450	18.4693(3)	20.9174(4)	22.2210(3)	14.9948(3)	15.9480(1)
$\beta$ , deg	90	96.3630(10)	61.3710(10)	92.1920(10)	94.8800(10)	96.28
vol, Å <sup>3</sup>	3946.74(4)	1786.73(5)	7564.3(3)	3104.22(8)	2701.27(9)	2674.33(4)
temp, °C	-80	-80	-80	-80	-80	-80
<i>R</i> <sub>1</sub> ( <i>F</i> <sub>o</sub> ), <i>wR</i> <sub>2</sub> ( <i>F</i> <sub>o</sub> <sup>2</sup> ) [ <i>F</i> <sub>o</sub> > 4σ( <i>F</i> <sub>o</sub> )]	0.0379, 0.0846	0.0310, 0.0673	0.0820, 0.2202	0.0824, 0.2479	0.0632, 0.1039	0.0519, 0.1051
<i>R</i> <sub>1</sub> ( <i>F</i> <sub>o</sub> ), <i>wR</i> <sub>2</sub> ( <i>F</i> <sub>o</sub> <sup>2</sup> ) [all data]	0.0474, 0.0895	0.0376, 0.0703	0.1249, 0.2442	0.1035, 0.2622	0.0938, 0.1133	0.0677, 0.1125
goodness of fit	1.096	1.046	1.088	1.045	1.112	1.099

(s), 143.93 (s), 138.39 (s), 137.02 (s), 133.14 (d, *J* = 35.5 Hz), 127.00 (br s), 124.41 (br s), 123.59 (s), 123.26 (s), 122.18 (s), 120.21 (s), 25.22 (d, *J* = 28.5 Hz), 23.95 (d, *J* = 17.9 Hz), 23.30 (d, *J* = 22.6 Hz), 22.05 (d, *J* = 20.3 Hz), 20.31–17.22 (m), 15.49 (br s), 14.96 (s). <sup>31</sup>P{<sup>1</sup>H} (THF-*d*<sub>8</sub>, -30 °C, 162 MHz): δ 74.23 (d, *J* = 7.9 Hz), 73.06 (d, *J* = 8.9 Hz). Anal. Calcd (found) for C<sub>27</sub>H<sub>42</sub>P<sub>2</sub>NiS: 62.45 (61.80) C; 8.15 (7.77) H.

**Preparation of (dippe)<sub>2</sub>Ni<sub>3</sub>(C<sub>13</sub>H<sub>10</sub>) (15):** Crystals of **15** were obtained by allowing a solution of **14** to stand in benzene for 3 weeks. <sup>1</sup>H NMR (400 MHz, THF-*d*<sub>8</sub>, 25 °C): δ 7.48 (d, *J* = 7.2 Hz, 1H), 7.36 (d, *J* = 7.2 Hz, 1H), 6.88 (d, *J* = 7.53, 1H), 6.75 (s, 1H), 6.49 (t, *J* = 7.3 Hz, 1H), 6.35 (t, *J* = 7.2 Hz, 1H), 6.23 (d, *J* = 7.4 Hz, 1H), 2.47 (s, 3H), 2.36 (oct, *J* = 7.0 Hz, 4H), 2.30 (oct, *J* = 6.7 Hz, 4H), 1.72–1.58 (m, 8H), 1.54–1.15 (m, 48H). <sup>31</sup>P{<sup>1</sup>H} (THF-*d*<sub>8</sub>, 25 °C, 162 MHz): δ 79.7 (br s).

**Preparation of (dippe)Ni(η<sup>2</sup>-C,S-1,9-dimethyldibenzothiophene) (19):** [(dippe)NiH]<sub>2</sub> (175 mg, 0.27 mmol) was added to a 2.38 g mixture of 4-methyldibenzothiophene (96%) and 1,9-dimethyldibenzothiophene (4%)<sup>35</sup> in 60 mL of hexanes and stirred at room temperature for 5 h. The orange-red precipitate **19** was collected by filtration and rinsed with pentane. Yield: 53 mg (22%). <sup>1</sup>H NMR (400 MHz, THF-*d*<sub>8</sub>, 25 °C): δ 7.36 (d, *J* = 7.5 Hz, 1H), 7.10 (t, *J* = 6.0 Hz, 1H), 6.80 (dt, *J* = 7.3, 1.5 Hz, 1H), 6.71 (t, *J* = 7.8 Hz, 1H), 6.65 (t, *J* = 7.4 Hz, 2H), 2.80 (oct, *J* = 7.2 Hz, 2H), 2.63 (oct, *J* = 7.2 Hz, 2H), 2.18 (s, 3H), 2.11–1.97 (m, 2H), 2.01 (s, 3H), 1.88–1.75 (m, 2H), 1.42–1.34 (m, 6H), 1.27 (dd, *J* = 14.0, 7.8 Hz, 3H), 1.17–1.10 (m, 9H), 0.77 (dd, *J* = 17.1, 7.3 Hz, 3H), 0.57 (dd, *J* = 14.6, 6.8 Hz, 3H). <sup>13</sup>C{<sup>1</sup>H} NMR (CD<sub>2</sub>Cl<sub>2</sub>, -70 °C, 100 MHz): δ 166.98 (br s), 148.89 (s), 143.84 (s), 140.93 (s), 134.26 (s), 131.56 (d, *J* = 2.9 Hz), 129.07 (d, *J* = 6.4), 127.34 (s), 125.31 (s), 124.72 (s), 124.54 (s), 123.14 (s), 25.13 (d, *J* = 28.0), 24.00 (d, *J* = 20.7 Hz), 22.53–21.74 (m), 20.24 (s), 20.13 (s), 19.97–19.78 (m), 17.92–17.40 (m), 16.21 (s), 15.79–15.59 (m), 15.39 (d, *J* = 6.4 Hz). <sup>31</sup>P{<sup>1</sup>H} (THF-*d*<sub>8</sub>, 25 °C, 162 MHz) δ 78.21 (d, *J* = 9.0 Hz), 74.95 (d, *J* = 9.3 Hz). Anal. Calcd (found) for C<sub>28</sub>H<sub>44</sub>NiP<sub>2</sub>S: 63.06 (62.91) C; 8.32 (8.57) H.

(35) 1,9-Dimethyldibenzothiophene was an impurity in the preparation of 4-methyldibenzothiophene. See ref 24.

**Preparation of (dippe)Ni(thioxanthene) (20):** [(dippe)NiH]<sub>2</sub> (81 mg, 0.13 mmol) was added to a hexanes (50 mL) solution of thioxanthene (200 mg, 1.0 mmol) and stirred at room temperature for 30 min. The mixture was then filtered, washed with hexanes, and dried leaving an orange solid (57 mg, 44%). <sup>1</sup>H NMR (400 MHz, THF-*d*<sub>8</sub>, 25 °C): δ 7.22 (dd, *J* = 7.2, 2.1 Hz, 1H), 7.14 (dd, *J* = 7.5, 5.7 Hz, 1H), 7.01 (dd, *J* = 6.9, 1.9 Hz, 1H), 6.74 (dt, *J* = 7.3, 1.7 Hz, 1H), 6.70–6.62 (m, 2H), 6.57 (t, *J* = 7.4 Hz, 1H), 6.50 (t, *J* = 7.1 Hz, 1H), 4.72 (d, *J* = 11.0 Hz, 1H), 3.79 (d, *J* = 11.0 Hz, 1H), 2.58–2.33 (m, 4H), 2.17–1.75 (m, 4H), 1.55–1.26 (m, 18 H), 1.10 (dd, *J* = 10.4, 6.8 Hz, 3H), 0.30 (dd, *J* = 13.2, 7.0 Hz, 3H). <sup>31</sup>P{<sup>1</sup>H} (THF-*d*<sub>8</sub>, 25 °C, 162 MHz): δ 71.97 (d, *J* = 15.3 Hz), 68.3 (d, *J* = 15.3 Hz). Anal. Calcd (found) for C<sub>27</sub>H<sub>42</sub>NiP<sub>2</sub>S: 62.45 (61.77) C; 8.15 (8.38) H.

**Preparation of (dippe)Ni(thianthrene) (21):** [(dippe)NiH]<sub>2</sub> (396 mg, 0.61 mmol) was added to a hexanes (70 mL) solution of thianthrene (600 mg, 2.8 mmol) and stirred at room temperature for 13 h. The mixture was then filtered and washed with hexanes. The crude material was recrystallized from benzene/hexanes leaving a yellow solid (299 mg, 46%). <sup>1</sup>H NMR (400 MHz, THF-*d*<sub>8</sub>, 25 °C): δ 7.47 (dd, *J* = 7.8, 1.6 Hz, 1H), 7.31 (dd, *J* = 7.8, 1.3 Hz, 1H), 7.00 (t, *J* = 7.2 Hz, 1H), 6.84–6.76 (m, 2H), 6.71 (dt, *J* = 7.2, 1.6 Hz, 1H), 6.60–6.55 (m, 2H), 2.76 (oct, *J* = 6.9 Hz, 2H), 2.59 (oct, *J* = 7.2 Hz, 2H), 2.20–1.84 (m, 4H), 1.67 (dd, *J* = 16.5, 7.5 Hz, 3H), 1.39–1.29 (m, 9H), 1.18–1.11 (m, 6H), 1.06 (dd, *J* = 14.0, 7.2 Hz, 3H), 0.27 (dd, *J* = 13.4, 7.2 Hz, 3H). <sup>31</sup>P{<sup>1</sup>H} (THF-*d*<sub>8</sub>, 25 °C, 162 MHz): δ 76.42 (d, *J* = 21.6 Hz), 72.34 (d, *J* = 21.6 Hz). Anal. Calcd (found) for C<sub>26</sub>H<sub>40</sub>NiP<sub>2</sub>S<sub>2</sub>: 58.11 (58.08) C; 7.50 (7.46) H.

**Preparation of [(dippe)Ni(μ-S)]<sub>2</sub> (24):** [(dippe)NiH]<sub>2</sub> (480 mg, 0.75 mmol) was added to a THF (60 mL) suspension of (dippe)Ni(SH)<sub>2</sub> (577 mg, 1.5 mmol) and stirred at room temperature for 24 h. The solution was then passed through a frit packed with a small amount of alumina. The solvent was removed on a vacuum line and the residue was recrystallized from THF–pentane to yield 335 mg (63%) of brown product. <sup>1</sup>H NMR (400 MHz, C<sub>6</sub>D<sub>6</sub>, 25 °C): δ 2.32 (oct, *J* = 5.9 Hz, 24 H), 1.63 (dd, *J* = 14.5, 7.1 Hz, 24 H), 1.08 (dd, *J* = 12.2, 7.0 Hz, 24 H), 0.99 (d, *J* = 10.0 Hz, 8H). <sup>13</sup>C{<sup>1</sup>H} NMR (C<sub>6</sub>D<sub>6</sub>, 25 °C, 100 MHz): δ 25.85–25.57 (m), 22.11 (quin, *J* = 9.0 Hz), 20.29 (s), 18.73

(s).  $^{31}\text{P}\{^1\text{H}\}$  (THF- $d_8$ , 25 °C, 162 MHz):  $\delta$  77.88 (s). Anal. Calcd (found) for  $\text{C}_{28}\text{H}_{64}\text{Ni}_2\text{P}_4\text{S}_2$ : 47.62 (47.36) C; 9.13 (9.24) H.

**Alternative preparations of 24 with R = c-hexyl:** (dcpe)Ni(Ph)-(SH) (75 mg) was heated in 2 mL of THF at 70 °C for 1.5 h upon which there was complete conversion to [(dcpe)Ni( $\mu$ -S)]<sub>2</sub>. NMR spectrum of [(dcpe)Ni( $\mu$ -S)]<sub>2</sub>:  $^1\text{H}$  NMR (400 MHz,  $\text{C}_6\text{D}_6$ , 25 °C):  $\delta$  2.51–1.18 (m, 48 H).  $^{31}\text{P}\{^1\text{H}\}$  (THF- $d_8$ , 25 °C, 162 MHz):  $\delta$  69.80 (s).

**General Description of X-ray Structural Determinations.** A single crystal of the compound was mounted on a glass fiber with Paratone-8277 (Exxon) oil. Data were collected at  $-80$  °C on a Siemens SMART CCD area detector system employing a 3 kW sealed tube X-ray source operating at 2.0 kW (50 kV, 40 mA). 1.3 hemispheres of data were collected over 6–13 h, which were then integrated using SAINT. Laue symmetry was used to confirm the crystal system, and cell parameters were determined from >2000 unique reflections.<sup>36</sup> The space group was assigned on the basis of systematic absences and intensity statistics using XPREP, and the structure solved using direct methods included in the SHELXTL 5.04 package. Data were corrected for absorption using the program SADABS.<sup>37</sup> In most final models, non-hydrogen atoms were refined anisotropically (full matrix on  $F^2$ ), with hydrogens

(36) It has been noted that the integration program SAINT produces cell constant errors that are unreasonably small, since systematic error is not included. More reasonable errors might be estimated at  $10\times$  the listed values.

included in idealized locations. Final residuals are reported for  $R_1$  and  $wR_2$ .<sup>38</sup> Selected crystallographic data are shown in Tables 1 and 2. Full descriptions of the structural solutions are given in the Supporting Information. ORTEP diagrams are shown with ellipsoids at the 30% probability level. Most hydrogen atoms are omitted for clarity.

**Acknowledgment** is made to the National Science Foundation (Grant CHE-9816365) for their support of this work. This paper is Dedicated to Professor Helmut Werner on the occasion of his 65th birthday.

**Supporting Information Available:** A listing of crystallographic information including data collection parameters, bond lengths, bond angles, fractional atomic coordinates, and anisotropic thermal parameters (PDF). This material is available free of charge via the Internet at <http://pubs.acs.org>.

JA9905997

(37) The SADABS program is based on the method of Blessing; see: Blessing, R. H. *Acta Crystallogr., Sect. A* **1995**, *51*, 33.

(38) Using the SHELXTL 5.04 package,  $R_1 = (\sum||F_o| - |F_c||)/\sum|F_o|$ ,  $wR_2 = [\sum[w(F_o^2 - F_c^2)^2]]$ .